RESEARCH LETTER

Combined scanning transmission X-ray and electron microscopy for the characterization of bacterial endospores

Jan Jamroskovic[1,2], Paul P. Shao[2], Elena Suvorova[2], Imrich Barak[1] & Rizlan Bernier-Latmani[2]

[1]Institute of Molecular Biology, SAS, Bratislava, Slovakia; and [2]Environmental Microbiology Laboratory of ENAC EPFL, Lausanne, Switzerland

Correspondence: Rizlan Bernier-Latmani, EML ENAC EPFL, Station 6, CH-1015 Lausanne, Switzerland.
Tel.: +41 21 693 5001;
fax: +41 21 693 6205;
e-mail: rizlan.bernier-latmani@epfl.ch

Received 30 May 2014; accepted 7 July 2014. Final version published online 12 August 2014.

DOI: 10.1111/1574-6968.12539

Editor: Simon Cutting

Keywords
Bacillus subtilis; DPA; EDS; sporulation; STEM; STXM.

Abstract

Endospores (also referred to as bacterial spores) are bacterial structures formed by several bacterial species of the phylum Firmicutes. Spores form as a response to environmental stress. These structures exhibit remarkable resistance to harsh environmental conditions such as exposure to heat, desiccation, and chemical oxidants. The spores include several layers of protein and peptidoglycan that surround a core harboring DNA as well as high concentrations of calcium and dipicolinic acid (DPA). A combination of scanning transmission X-ray microscopy, scanning transmission electron microscopy, and energy dispersive spectroscopy was used for the direct quantitative characterization of bacterial spores. The concentration and localization of DPA, Ca^{2+}, and other elements were determined and compared for the core and cortex of spores from two distinct genera: *Bacillus subtilis* and *Desulfotomaculum reducens*. This micro-spectroscopic approach is uniquely suited for the direct study of individual bacterial spores, while classical molecular and biochemical methods access only bulk characteristics.

Introduction

Bacterial sporulation is the process of endospore formation associated with members of bacterial phylum Firmicutes. A number of genera such as *Bacillus*, *Clostridium*, and *Desulfotomaculum* include species able to sporulate. Some are pathogenic such as *Bacillus anthracis, B. cereus, Clostridium difficile, C. botulinum, and C. perfrigens*, while others are not (e.g. *B. subtilis*, *C. acetobutylicum*, and *Desulfotomaculum reducens*).

Bacillus subtilis sporulation is an example of a simple cell differentiation process and has been studied for decades. One of the first morphological changes due to sporulation is the formation of an asymmetrically positioned sporulation septum that divides the cell into two compartments – a larger mother cell and a smaller forespore. This process is followed by engulfment of the forespore within the mother cell. The spore is then gradually dehydrated and accumulates dipicolinic acid (DPA) and metal ions, particularly Ca^{2+}. The synthesis of DPA is mediated in the mother cell at late sporulation stages by the proteins SpoVFA and SpoVFB (Daniel & Errington, 1993), and DPA is subsequently taken up into the forespore via channels consisting of SpoVA proteins (Li *et al.*, 2012). The absence of DPA in spores causes changes in spore resistance to various physical and chemical agents (Paidhungat *et al.*, 2002). The cortex and spore coat are formed while the spore is within the mother cell. After completion of the sporulation process, the mother cells lyse and release the complete spore (Henriques & Moran, 2007). The seven stages of sporulation are tightly controlled by sporulation-specific sigma transcription factors, which are activated in concert with morphological changes of the mother cell and forespore. Once released, the spore can survive harsh conditions, including high temperatures, desiccation, and chemical toxicants. It is also able to germinate in hours once the conditions return to a range viable for vegetative cells.

The study of sporulation and germination has been ongoing for decades and has relied primarily on molecular tools to unravel the complex series of biochemical processes that ultimately lead to the formation of a mature spore. While it is undeniable that this approach has been extremely effective at uncovering details of the overall process, it remains that it relies on bulk characterization of a given culture. Hence, it has limited usefulness when the

FEMS MICROBIOLOGY LETTERS

question requires localization of specific chemical components within the sporulating cell or the spore. Thus, for the study of the transport and localization of metal and DPA in the cell and the spore, such bulk approach is unsuitable. In this work, we combine two microscopy techniques, scanning transmission electron microscopy (STEM) coupled to energy dispersive spectroscopy (EDS) and scanning transmission X-ray microscopy (STXM), to allow the direct study of the localization of DPA, calcium, and other metals in the bacterial cells and spores. To demonstrate the potential of this combination of tools, we characterized the distribution of metals and DPA in the spores of two distinct genera, the anaerobic bacterium *D. reducens* and the aerobic bacterium *B. subtilis*.

Materials and methods

Media and bacterial growth

Bacillus subtilis strains used in the study are derived from strain *B. subtilis* PY79. The *B. subtilis* Δ*spoV*F Δ*sle*B mutant strain was prepared by sequential transformation of chromosomal DNA of strains *B. subtilis spoVF::tet* (Paidhungat *et al.*, 2001) and *B. subtilis sleB::spc* (Paidhungat *et al.*, 2001) into *B. subtilis* PY79 strain selected on tetracycline and spectinomycin resistance, respectively.

Wild-type (WT) strain *B. subtilis* PY79 (Youngman *et al.*, 1984) and mutant strain *B. subtilis* Δ*spoV*F Δ*sle*B were inoculated into liquid Difco sporulation medium (DSM, Schaeffer *et al.*, 1965) at $OD_{600\ nm} = 0.1$ using overnight-plated bacteria as an inoculum. The cultures were grown at 37 °C with rotational shaking at 150 r.p.m. After 48 h, samples were centrifuged at 10 000 ***g*** for 10 min. Supernatants were carefully discarded, and bacterial pellets washed three times by deionized cold water to remove the medium and stored in deionized water at 4 °C. Both samples consisted of more than 90% spores.

Desulfotomaculum reducens strain MI-1 was grown anaerobically in liquid basal Widdel low-phosphate medium (pH 7.1) supplemented with trace elements and vitamins (Bernier-Latmani *et al.*, 2010) and 20 mM sulfate and 10 mM lactate. After several days of incubation at 37 °C, the culture was centrifuged at 10 000 ***g*** for 10 min. The supernatant was carefully discarded, and the bacterial pellet washed three times in deionized cold water to remove the medium and stored in deionized water at 4 °C. The sample consisted of more than 50% spores.

Sample preparation

Samples (1.0–5.0 μL) were loaded on carbon grids (Lacey Carbon support grids, EMS) or on silicon nitride (SiNi) microporous or nonporous TEM window grids (TEM windows). After 1–5 min, excess liquid was wicked away with filter paper. Silicon nitride (SiNi) microporous or nonporous TEM window grids (TEMwindows, West Henrietta, NY) were mounted on STXM holders with double-sided sticky carbon or conventional tape. The use of epoxy to affix the grids was found to significantly contribute to contaminant aromatic signals at *c.* 285 eV (not shown) and was discontinued. Samples (1.0 μL) were loaded on the SiNi window and allowed to settle for 5 min before excess liquid was wicked away. The distribution of the adhered sample was observed by light microscopy prior to transfer to the beamline. Ideally, the sample would be relatively sparsely distributed across the window. Dense concentration led to salt crystal formation or difficulty penetrating the sample with the beam. Too little adhered sample resulted in significant searching for areas of interest, an inefficient use of beam time. Sample mounted on SiNi grids was first used for STXM microscopy and subsequently for STEM-EDS. It is important to note that the ability to use whole mount samples for STEM/STXM analysis is a feature for the detection of metal and specific carbon-containing compounds in the spore. Thin sections would not allow the detection of DPA by STXM due to the weakness of the signal.

STXM data collection and processing

STXM beamtime was conducted at the STXM end station, part of the SM beamline at the Canadian Light Source (CLS). The 250-line mm^{-1} low energy grating and 25-μm exit slit were used for carbon K-edge imaging and spectroscopy. Carbon K-edge energy calibration was accomplished using the 3p Rydberg peak at 294.96 eV of gaseous CO_2 (Rieger *et al.*, 1986). Carbon speciation stacks were collected through serial image collection along C K-edge energies (280 – 300 eV) extended to capture the calcium L_{II} and L_{III} edge peaks; thus, the entire energy range considered was 280–355 eV. Experiment-specific standards included: DPA, calcium carbonate, Ca–DPA complex (obtained by mixing the two solutes), and peptidoglycan. Spectra for standards were collected using line scans through regions of sample with thicknesses that allowed for roughly one-half maximum transmission. All the spectra were normalized to an optical density (OD) corresponding to a 1-nm layer. Data processing was done using the AXIS2000 software package (Hitchcock, 1997). Stacks were iteratively aligned to convergence by cross-correlation using the Jacobsen stack analyze algorithm (Jacobsen *et al.*, 2000) with the highest energy image as a reference. Quantitative C-speciation maps were calculated from the aligned image stacks by singular value decomposition using the stack-fit routine

in AXIS2000. Spectra were initially evaluated and normalized to 1-nm thickness using AXIS2000 before importing into Excel for direct data manipulation. Compared spectra were scaled linearly using 280 eV and 289.2 eV as endpoints for the carbon spectra and 346 eV and 356 eV for Ca spectra. To decrease the noise of the data, principle component analysis (PCA) was used (Malinowski, 1991). Spectra for each pixel were divided into different clusters by cluster analysis (Everitt *et al.*, 2001) depending on their similarities.

STEM/EDS data collection and processing

STEM with X-ray energy dispersive spectrometry (EDS) was used to obtain elemental composition maps and to perform comparative characterization of elemental content. In this study, an X-ray EDS system (Esprit/Quantax Bruker) in STEM mode in a FEI Tecnai Osiris microscope (200 kV X-FEG field emission gun, X-ray detector (Super-X) with 4 × 30 mm^2 windowless SDD diodes and 0.9sr collection angle at 22° take-off angle) was applied. Quantitative EDS analysis was carried out using the Cliff-Lorimer standard-less method with thickness correction using K-series. The physical Bremsstrahlung background was calculated based on the sample composition. Some elements such as Cu contributing from the Cu grid or Si and N coming from the silicon nitride support were removed from quantification after the deconvolution procedure in the quantification process. Elemental concentrations in atomic % and net counts (signal above background) were derived from deconvoluted line intensities within a 95% confidence level. The process time and acquisition rates were adapted to get the most accurate data for specific element such as Ca, P, and Mn. The experimental spectra were collected with no pile-up artifacts. A correction for specimen drift was applied during acquisition to improve elemental mapping accuracy.

Results and discussion

Energy dispersive X-ray spectroscopy is a high-energy technique, typically used on hard materials that are resilient to the bombardment required to eject a sufficient number of electrons to get a statistically significant X-ray count. However, in this system, the four windowless Super-X SDD EDX detectors integrated into the pole piece have such sensitivity that we could decrease the amount of incident radiation needed to use this method on intact soft biological materials. Thus, this technique allows the acquisition of elemental maps from bacterial endospores and cells.

High-angle annular dark field (HAADF) STEM revealed the ability to capture images of *B. subtilis* endospores that clearly show the structure of an electron dense core surrounded by a less dense cortex and coat (Fig. 1a). This is highly informative because these are whole mount samples and imaging in this manner allows rapid discrimination of spores and cells.

We gain further insight when the region is mapped by EDS (Fig. 1b). The localization of Ca is clearly inside the spore core, and the main contribution of P is in cortex and coat regions (Fig. 1b). To confirm the Ca distribution inside the spores, a cross section of the concentration of Ca, P, and Mn is shown in Fig. 1c. Thus, the bell-shaped calcium concentration profile indicates an increase in Ca atomic percent in the center of the spore, which corresponds to the spore core.

With this technique, imaging of the spores and their discrimination from vegetative cells is performed on a routine basis. Additionally, calcium localization is readily obtained by EDS. However, because the techniques only collect images and the elemental composition of the sample, no specific information about the composition of the sample can be retrieved.

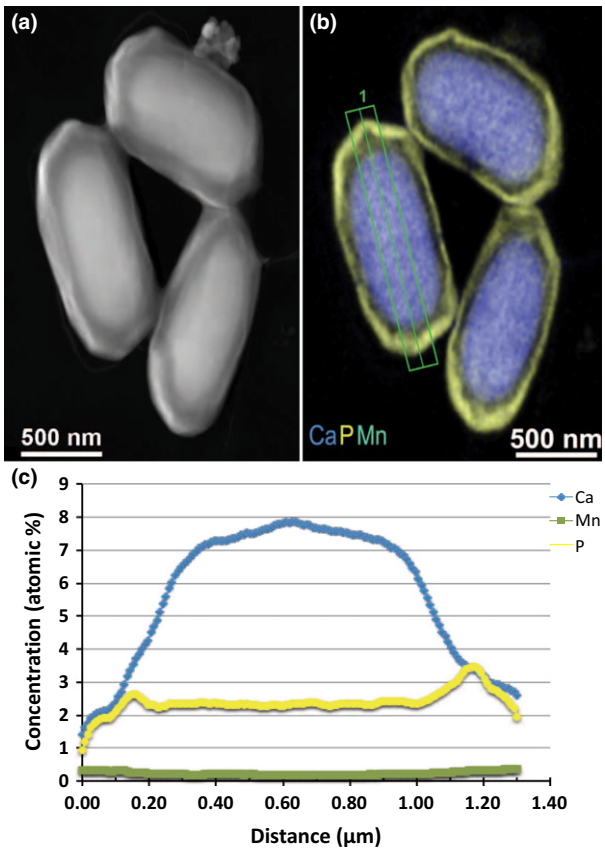

Fig. 1. (a) STEM/EDS imaging (HAADF) of *Bacillus subtilis* spores showing the core and cortex/coat. (b) Spatial distribution of Ca, Mn, and P. (c) Elemental distribution along the line (labeled 1) is shown in the corresponding graph.

In contrast, STXM, which is a synchrotron-based spectro-microscopy, enables the identification of biomolecules by their spectra along the carbon K-edge energy range. The incident beam passes through the sample and varies its intensity based on the composition at the point of passage. Depending on the specific biomolecule present, the C absorption spectrum will vary, allowing the fingerprinting of specific molecules. This is useful because we can differentiate one carbon-containing biomolecule from another. As this technique is also a scanning technique, a given sample can have its biomolecules mapped by raster scanning a region and modulating the energy to build a 'stack' of images, each image collected at a particular energy. This information can be computationally reconstructed so that each pixel can have biomolecule components assigned to it based on the spectra collected at that pixel. Altogether, this allows mapping of the distribution of given biomolecules.

When examining sporulation, a vital component is DPA, which is packaged in the core of the spore and is believed to contribute to their ability to resist harsh environments (Paidhungat *et al.*, 2002). We show that the DPA standard has a double peak at 284.7 and 285.35 eV (Fig. 2a). However, the first peak is also characteristic of other aromatic

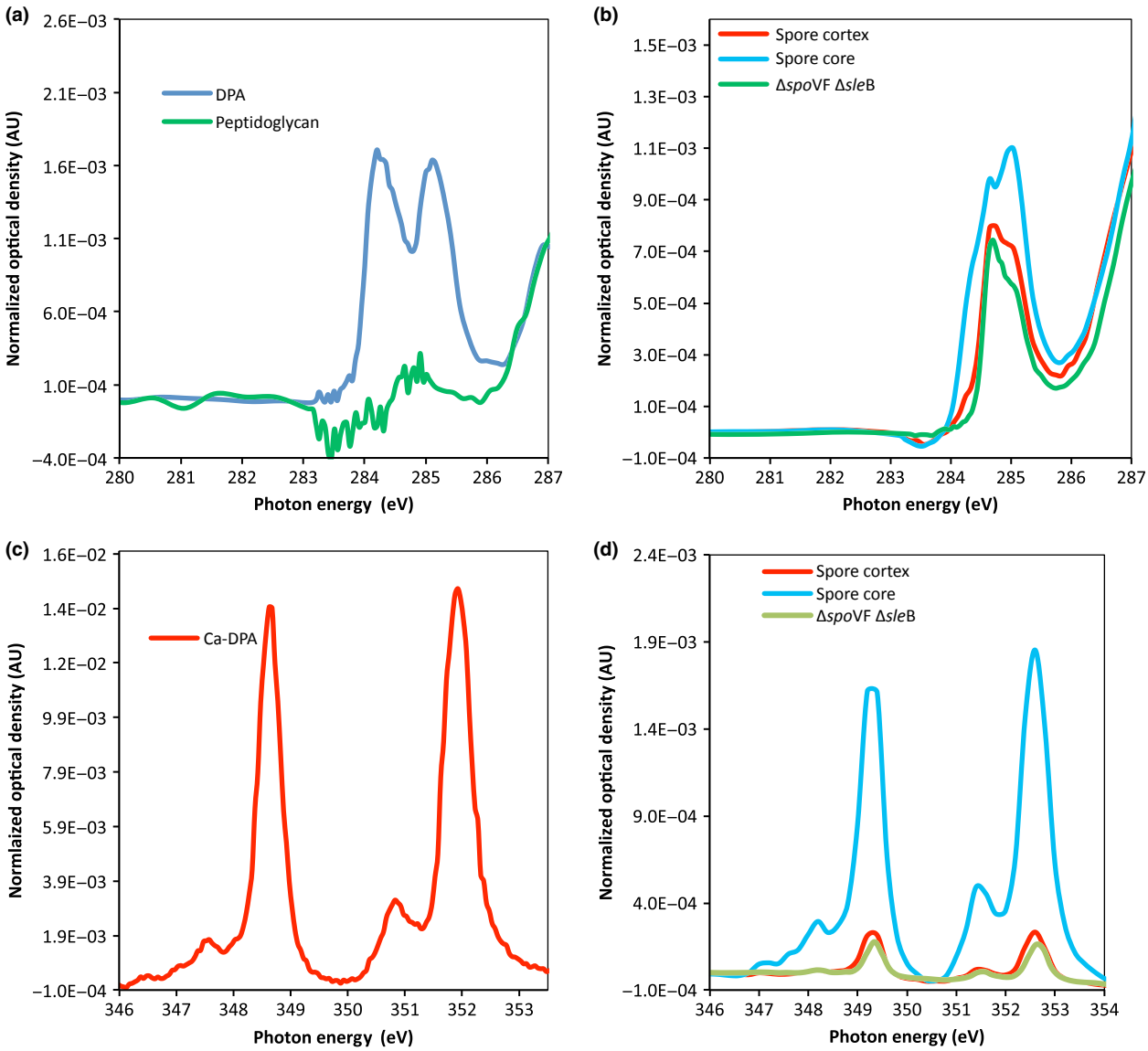

Fig. 2. (a) C K-edge absorption spectra for two standards: DPA and peptidoglycan; (b) absorption spectra at the C K-edge for WT spores core, cortex, and spores core of Δ*spo*VF Δ*sle*B mutants; (c) Ca L-edges absorption spectra for the standard Ca-DPA, and (d) for WT spores core, cortex and spores core of Δ*spo*VF Δ*sle*B mutants. Spectra are normalized to 1-nm thickness.

groups such as tyrosine. Hence, only the second peak at 285.35 eV is truly characteristic of DPA. As long as our data are collected at fine enough energy steps to resolve the two peaks, we can positively identify DPA localization. We compared the C K-edge spectrum for the core and cortex of a WT spore and observed the presence of the second peak in the spore core of the *B. subtilis* WT strain but not in the cortex (Fig. 2b). Thus, we were able to confirm the expected localization of DPA.

As a negative control for DPA presence, we used spores of the *B. subtilis* Δ*spoVF* Δ*sleB* mutant strain, which is not capable of DPA synthesis (Fig. 2b). After analysis, a single peak was observed at 284.7 eV in both regions (core and cortex) of the spore. The other peak at 285.35 eV, which is characteristic of the presence of DPA, was missing.

At these soft X-ray energies, we are also able to localize calcium according to its L_{II} and L_{III} edges. Our calcium–DPA complex standard showed peaks at 349.0 and 352.0 eV with shoulders just to the left of each peak that may potentially give information about its complexation (Fig. 2c). The calcium peaks were observed also in region of *B. subtilis* spore core. Calcium peaks in the spore cortex of *B. subtilis* WT strain and core of *B. subtilis* Δ*spoVF* Δ*sleB* mutant were four times lower than calcium peaks in the WT strain, which means a fourfold greater calcium concentration in the WT spore core as compared to the WT spore cortex and the Δ*spoVF* Δ*sleB* mutant spore core (Fig. 2d).

When using a combination of the two techniques on a single sample, it is possible to acquire information about the localization of DPA and calcium, that of other

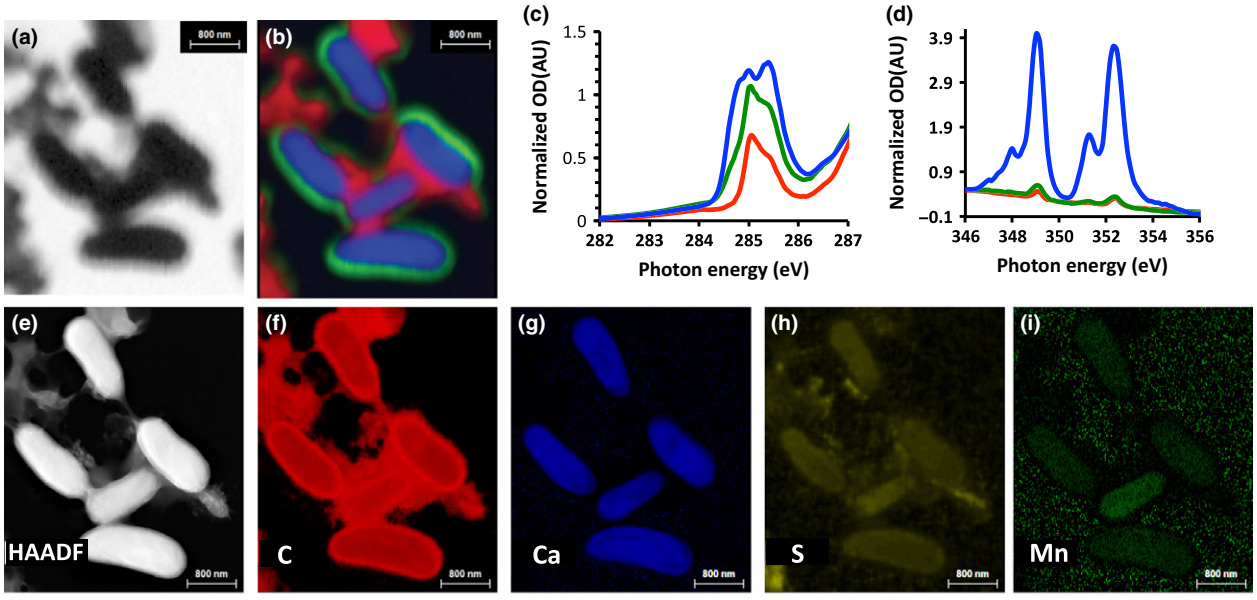

(k)

	Atomic percent									
	C	O	Na	Mg	P	S	Cl	Ca	Mn	Fe
1	72.85	16.01	0.04	0.21	1.15	1.47	0.06	7.79	0.25	0.16
2	77.56	11.68	0.02	0.29	1.44	1.46	0.09	6.86	0.49	0.11
3	72.64	16.81	0.05	0.24	1.26	1.34	0.07	7.23	0.22	0.15
4	74.72	14.96	0.05	0.24	1.18	1.31	0.09	7.12	0.22	0.12
5	73.91	15.64	0.07	0.29	1.34	1.09	0.07	7.23	0.26	0.11
6	76.67	15.18	0.17	0.16	2.58	1.80	0.29	0.39	0.00	2.76
7	85.46	11.09	0.08	0.11	0.65	1.70	0.35	0.09	0.02	0.44

Fig. 3. Combined STXM–STEM/EDS of identical region of spores of *Desulfotomaculum reducens*. (a) STXM picture acquired at 288.2 eV. Stack energy was collected at carbon K-edge extended to calcium L_{II} and L_{III} edges. (b) RGB map of the STXM energy stack deconvoluted into three components corresponding to spore core (blue), spore cortex (green), and cell debris (red). (c) STXM energy spectra for carbon K-edge and (d) STXM energy spectra for calcium L-edges of the three components: spore core (blue), spore cortex (green), and cell debris (red). (e) STEM HAADF image of same region taken after STXM data collection. (f–i) EDS elemental maps for C, Ca, S, and Mn, respectively. Ca is characteristically restricted to the core. (j) Combined EDS elemental map for P, Ca, Mn, and Fe. Circles with numbers represent regions of interest whose elemental composition (in atomic percent) is shown in the table (k).

elements (e.g. S, N, Mg, K, Mn) as well as an image of the morphology of the forespore in different stage of development or in the whole spore. STXM must be applied first to capture the speciation of carbon, allowing the identification of the localization of DPA (Fig. 3a, b and c). Additionally, by probing the calcium energy region (346–355 eV), the calcium signal from the spore can also be mapped (Fig. 3d). Subsequently, the same sample can be imaged by STEM coupled to EDS. STEM HAADF imaging reveals the morphology of the spore (Fig. 3e). In contrast to STXM imaging (Fig. 3a), the cortex and the core are clearly delineated in the STEM image (Fig. 3e). Additionally, elemental mapping of the spore is achieved using EDS in scanning transmission mode in the microscope (Fig. 3f–i). The EDS map and table clearly show the concentration of calcium in the core rather than the cortex region (Fig. 3j and k). The table lists the atomic percent of relevant elements at specific regions of interest within the sample. Carbon and oxygen are dominant (due to the carbon-coated grid), but there are large differences in Ca content depending on the location within the sample, illustrating the accumulation of Ca in the spore core.

The power of combining these techniques stems from simultaneously characterizing the localization of heavier elements relevant to sporulation (e.g. Ca, K) and that of carbon-containing biomolecules such as DPA. Using this combination, detailed studies of the mechanism of accumulation of DPA and Ca in the spore core as well as probing studies of the distribution of DPA, Ca, and/or metals in less well-studied spore-forming microorganisms such as *Clostridium* species are possible.

The net advantage that this combined approach holds over conventional biomolecular approaches used to date is that it allows the observation of the intracellular localization of both DPA and calcium in individual cells. To study the mechanism of calcium or DPA accumulation in the spore or to evaluate the role of other metals in sporulation, bulk approaches do not provide the spatial resolution necessary to pinpoint the processes at play. Hence, STXM and STEM-EDS provide a novel and powerful complement to the molecular tools in use in the field of sporulation research.

Acknowledgements

The work was funded by a Swiss Government Excellence Fellowship to J.J. (Fellowship # 2013.0198). It was also supported by grant from SAS (2/0009/13) and by a grant from the Slovak Research and Development Agency (APVV-00335-10).

References

Bernier-Latmani R, Veeramani H, Vecchia ED, Junier P, Lezama-Pacheco JS, Suvorova EI, Sharp JO, Wigginton NS & Bargar JR (2010) Non-uraninite products of microbial U(VI) reduction. *Environ Sci Technol* **44**: 9456–9462.

Daniel RA & Errington J (1993) Cloning, DNA sequence, functional analysis and transcriptional regulation of the genes encoding dipicolinic acid synthetase required for sporulation in *Bacillus subtilis*. *J Mol Biol* **232**: 468–483.

Everitt BS, Landau S & Leese M (2001) *Cluster Analysis*, 4th edn. Arnold Publishers London.

Henriques AO & Moran CP (2007) Structure, assembly, and function of the spore surface layers. *Annu Rev Microbiol* **61**: 555–588.

Hitchcock AP (1997) AXIS2000 software, last version 2013, available from http://unicorn.mcmaster.ca/aXis2000.html/

Jacobsen C, Wirick S, Flynn G & Zimba C (2000) Soft X-ray spectroscopy from image sequences with sub-100 nm spatial resolution. *J Microsc* **197**: 173–184.

Li Y, Davis A, Korza G, Zhang P, Li YQ, Setlow B, Setlow P & Hao B (2012) Role of a SpoVA protein in dipicolinic acid uptake into developing spores of *Bacillus subtilis*. *J Bacteriol* **194**: 1875–1884.

Malinowski ER (1991) *Factor Analysis in Chemistry*, 2nd edn. John H. Wiley & Sons, New York, NY.

Paidhungat M, Ragkousi K & Setlow P (2001) Genetic requirements for induction of germination of spores of *Bacillus subtilis* by Ca(2+)-dipicolinate. *J Bacteriol* **183**: 4886–4893.

Paidhungat M, Setlow B, Driks A & Setlow P (2002) Characterization of spores of *Bacillus subtilis* which lack dipicolinic acid. *J Bacteriol* **182**: 5505–5512.

Rieger D, Himpsel FJ, Karlsson UO, McFeely FR, Morar JF & Yarmoff JA (1986) Electronic-structure of the CAF_2/Si (111) interface. *Phys Rev B Condens Matter* **34**: 7295–7306.

Schaeffer P, Millet J & Aubert JP (1965) Catabolic repression of bacterial sporulation. *P Natl Acad Sci USA* **54**: 704–711.

Youngman P, Perkins JB & Losick R (1984) Construction of a cloning site near one end of Tn917 into which foreign DNA may be inserted without affecting transposition in *Bacillus subtilis* or expression of the transposon-borne *erm* gene. *Plasmid* **12**: 1–9.